The set of diagnostics for the first operation campaign of the Wendelstein 7-X stellarator

Citation for published version (APA):
König, R., Baldzuhn, J., Biel, W., Biedermann, C., Bosch, H. S., Bozhenkov, S., Braeuer, T., Brotas de Carvalho, B., Burhenn, R., Buttenschoen, B., Cseh, G., Czarnecka, A., Endler, M., Erckmann, V., Estrada, T., Geiger, J., Grulke, O., Hartmann, D., Hathiramani, D., ... Zoletnik, S. (2015). The set of diagnostics for the first operation campaign of the Wendelstein 7-X stellarator. *Journal of Instrumentation*, *10*, 1-17. Article P10002. https://doi.org/10.1088/1748-0221/10/10/P10002

DOI:
10.1088/1748-0221/10/10/P10002

Document status and date:
Published: 01/10/2015

Document Version:
Publisher's PDF, also known as Version of Record (includes final page, issue and volume numbers)

The Set of Diagnostics for the First Operation Campaign of the Wendelstein 7-X Stellarator

2015 JINST 10 P10002

(http://iopscience.iop.org/1748-0221/10/10/P10002)

Published by IOP Publishing for Sissa Medialab

Received: *May 26, 2015*
Accepted: *August 3, 2015*
Published: *October 2, 2015*

1st EPS Conference on Plasma Diagnostics (1stECPD)
14–17 April 2015
Frascati, Rome, Italy

The Set of Diagnostics for the First Operation Campaign of the Wendelstein 7-X Stellarator

Ralf König,[a,1] J. Baldzuhn,[a] W. Biel,[b] C. Biedermann,[a] H.S. Bosch,[a] S. Bozhenkov,[a] T. Bräuer,[a] B. Brotas de Carvalho,[c] R. Burhenn,[a] B. Buttenschön,[a] G. Cseh,[d] A. Czarnecka,[e] M. Endler,[a] V. Erckmann,[a] T. Estrada,[f] J. Geiger,[a] O. Grulke,[a] D. Hartmann,[a] D. Hathiramani,[a] M. Hirsch,[a] S. Jabł onski,[e] M. Jakubowski,[a] J. Kaczmarczyk,[e] T. Klinger,[a] S. Klose,[a] G. Kocsis,[d] P. Kornejew,[a] A. Krämer-Flecken,[b] T. Kremeyer,[g] M. Krychowiak,[a] M. Kubkowska,[e] A. Langenberg,[a] H. P. Laqua,[a] M. Laux,[a] Y. Liang,[b] A. Lorenz,[a] A.O. Marchuk,[b] V. Moncada,[h] O. Neubauer,[b] U. Neuner,[a] J.W. Oosterbeek,[i] M. Otte,[a] N. Pablant,[j] E. Pasch,[a] T.S. Pedersen,[a] K. Rahbarnia,[a] L. Ryc,[e] O. Schmitz,[g] W. Schneider,[a] H. Schuhmacher,[k] B. Schweer,[b] T. Stange,[a] H. Thomsen,[a] J.-M. Travere,[h] T. Szepesi,[d] U. Wenzel,[a] A. Werner,[a] B. Wiegel,[k] T. Windisch,[a] R. Wolf,[a] G.A. Wurden,[l] D. Zhang,[a] A. Zimbal,[k] S. Zoletnik[d] and the W7-X Team

[a]*Max Planck Inst. for Plasma Physics, 17491 Greifswald, Germany*
[b]*Institute of Energy- and Climate Research, Forschungszentrum Jülich GmbH, D-52425 Jülich, Germany*
[c]*Instituto de Plasmas e Fusao Nuclear Instituto Superior Tecnico, Lisbon, Portugal*
[d]*Wigner Research Centre for Physics, Konkoly Thege 29-33, H-1121 Budapest, Hungary*
[e]*IFPiLM, Hery Street 23, 01-497 Warsaw, Poland*
[f]*Laboratorio Nacional de Fusi'on, CIEMAT, Avenida Complutense, Madrid, Spain*
[g]*Univ. of Wisconsin, Dept. of Engineering Physics, 1500 Engineering Drive, Madison, WI 53706*
[h]*CEA, IRFM, F-13108 Saint-Paul-lez-Durance, France*
[i]*Eindhoven University of Technology, P.O. Box 513, 5600 MB Eindhoven, The Netherlands*
[j]*Princeton Plasma Physics Laboratory, Princeton, New Jersey 08543, U.S.A.*
[k]*Physikalisch-Technische Bundesanstalt, Bundesallee 100, 38116 Braunschweig, Germany*
[l]*Los Alamos National Laboratory, Los Alamos, NM 87544, U.S.A.*

E-mail: Ralf.Koenig@ipp.mpg.de

[1]Corresponding author.

doi:10.1088/1748-0221/10/10/P10002

ABSTRACT: Wendelstein 7-X (W7-X) is a large optimized stellarator (B=2.5T, V=30m^3) aiming at demonstrating the reactor relevance of the optimized stellarators. In 2015 W7-X will begin its first operation phase (OP1.1) with five inertially cooled inboard limiters made of graphite. Assuming the heat loads can be spread out evenly between the limiters, 1 second discharges at 2 MW of ECRH heating power could be run in OP1.1. The expected plasma parameters will be sufficient to demonstrate the readiness of the installed diagnostics and even to run a first physics program. The diagnostics available for this first operation phase, including some special limiter diagnostics, and their capabilities are being presented.

A shorter version of this contribution is due to be published in PoS at:
1st EPS conference on Plasma Diagnostics

KEYWORDS: Plasma diagnostics - probes; Nuclear instruments and methods for hot plasma diagnostics; Plasma diagnostics - interferometry, spectroscopy and imaging

Contents

1 Introduction

The Wendelstein 7-X (W7-X) stellarator [1–3] with its superconducting coil system will be taken towards one of its central aims of demonstrating quasi-continuous plasma operation in three steps. For the upcoming very first plasma operation phase OP1.1 five inertially cooled inboard limiters made of graphite have been installed. These will, in the run-up to OP1.2, which starts one year later, be exchanged by 10 inertially cooled test divertor units (TDU). The shape of the TDU exactly mimics the actively cooled high heat flux (HHF) divertor, which will finally be available for pushing

2015 JINST 10 P10002

to quasi-continuous operation with the beginning of OP2, currently foreseen to start in 2019. With very few exceptions, all installed diagnostics are already suitably hardened for this later, highly demanding, high heating power ($P_{\mathrm{ECRH}} \sim 10\,\mathrm{MW}$), quasi-continuous operation phase [4–6]. However, hardening the diagnostics with respect to the effect of neutrons and γ-rays will only be taken care of in preparation for OP2, since deuterium operation is only foreseen from OP2 onward. The maximum total number neutrons per year will be limited to $3\,10^{19}$, e.g. corresponding to about 500 NBI heated pulses of 10 s duration at maximum expected neutron rate. In general W7-X is expected to be mainly operated in hydrogen since no distinct isotopic effect has been observed in W7-AS [7].

The presently ongoing commissioning of W7-X has started in May 2014 with the closure of the cryostat. The installation of the in-vessel components has been completed by the end of last year. At the beginning of March 2015 the leak testing of the plasma vessel has started and the cool down to less than 4 K been successfully demonstrated, so that the commissioning of the magnet system can now begin in early May 2015. This demonstrates that starting the first plasma operation period of 13 weeks duration in early autumn this year seems realistic. The main aim of OP1.1 is to enable an early commissioning and demonstration of the safe system operation of the main W7-X device systems, like vacuum, vessel conditioning (baking, helium glow discharge cleaning), cryogenics, magnetic field coils and the ECRH heating. Of course this phase will also be used for commissioning and testing of most of the diagnostics required for OP1.2, albeit many of them being not yet fully integrated into the standard W7-X data acquisition and control system at this stage.

The brief first campaign OP1.1 will also be used to perform some very first physics experiments [8]. With the carbon tiles not yet attached to the heat shields and the already installed divertor frame being unprotected, particular care has been taken in designing a limiter magnetic configuration which ensures that these components are not exposed to any convective loads. With the limiters being simply attached to the heat shield structures we expect to be able to run 1 second discharges at 2 MW of heating power (ECRH), assuming the heat loads can be spread out evenly across the limiters. The plasma parameters expected to be achievable under these conditions ($T_e < 3.5\,\mathrm{keV}$, $T_i < 0.9\,\mathrm{keV}$, $n_e < 2\ 10^{19}\,\mathrm{m}^{-3}$) are expected to be sufficient to demonstrate the readiness of the installed diagnostics and even to run a small first physics program, initially with helium and possibly even a few weeks with hydrogen. In order to enable the short physics program, a group of 8 high priority diagnostics essential for OP1.1 had been defined. This set of essential diagnostics consists of the neutron counters (safety regulator requirement, only hydrogen plasma in OP1.1), the flux surface measurements to demonstrate that the magnetic field accuracy has been achieved, the interferometer, ECE and video diagnostic for basic plasma parameter determination and monitoring, and the basic limiter diagnostics, like the limiter thermo-couples, the limiter Langmuir probes and the limiter infrared/visible observation systems, to allow some first SOL physics experiments. A further group of 16 diagnostics expected but not guaranteed to be ready for OP1.1 had also been defined. The complete set of both groups of diagnostics have been installed on W7-X in time for OP1.1 and are being reported on in this paper. A further set of approx. 20 diagnostics not described here require longer completion times or are directly connected to the TDU divertor and therefore will only be completed in time for OP1.2.

2 Diagnostic for OP1.1

Figure 1 shows for one of the 5 modules of W7-X the location of the port types available for diagnostics. In the other modules the port locations are mostly identical, only few ports have a slightly different shape and orientation.

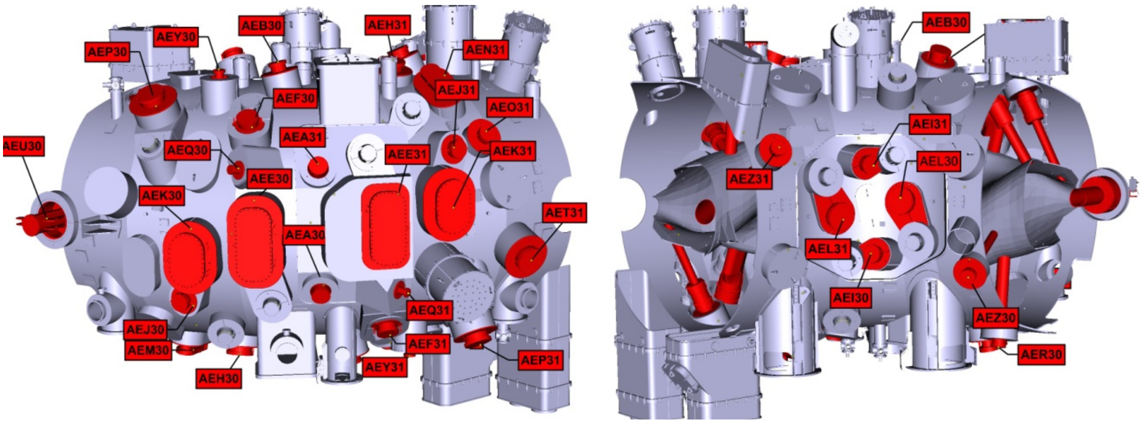

Figure 1. Diagnostics ports in half modules 30/31: left figure outer view, right figure view from torus centre.

2.1 Photo documentation of all in-vessel components

The assembly of the in-vessel components has been documented following the W7-X Quality Assembly and Assurance plans. According to these rules the names/numbers, geometric positions of components, as well as the achieved quality of welds, the results of leak and insulation checks and many other tests were documented. Due to the high complexity of the in-vessel installations, in addition, a complete photo documentation has been compiled. This photo documentation aimed at gaining at least a rough position determination of non-surveyed components, like flexible hoses, cable trays, etc., the geometric relation between neighbouring components (gaps) and the (virgin) colour of the components before having been exposed to plasma. The documentation will allow first analysis in case of possible in-vessel component faults/damages and looking for effects the plasmas of the first operation phase may have had on the in-vessel components.

The requirements on the photo documentation were kept simple: a) 95% of the vacuum vessel surface has been covered, b) a resolution of the panorama images of better than 2 pxl/mm has been achieved and c) a colour resolution aimed at, which is expected to allow detection of surface discolouring induced by plasma operation. For the photo documentation panorama images of $360^\circ \times 175^\circ$ were created at 6 positions in each module. A Nikon 810 camera equipped with a $f = 20\,\text{mm}$ lens and mounted on a motorized, fully automatic panorama head was used to take 3×9 images with approx. 30% overlap to create a single panorama. At each camera position 3 pictures were taken, with exposure times equivalent to -2, 0, $+2$ stops, to achieve optimal results. The main challenge in taking the panorama images was the illumination of the vacuum vessel. The best results were achieved by combining the standard illumination used for assembly work with a mobile LED-photo lamb (1200 lux at 1 m) fixed to the camera. Each panorama image has a size

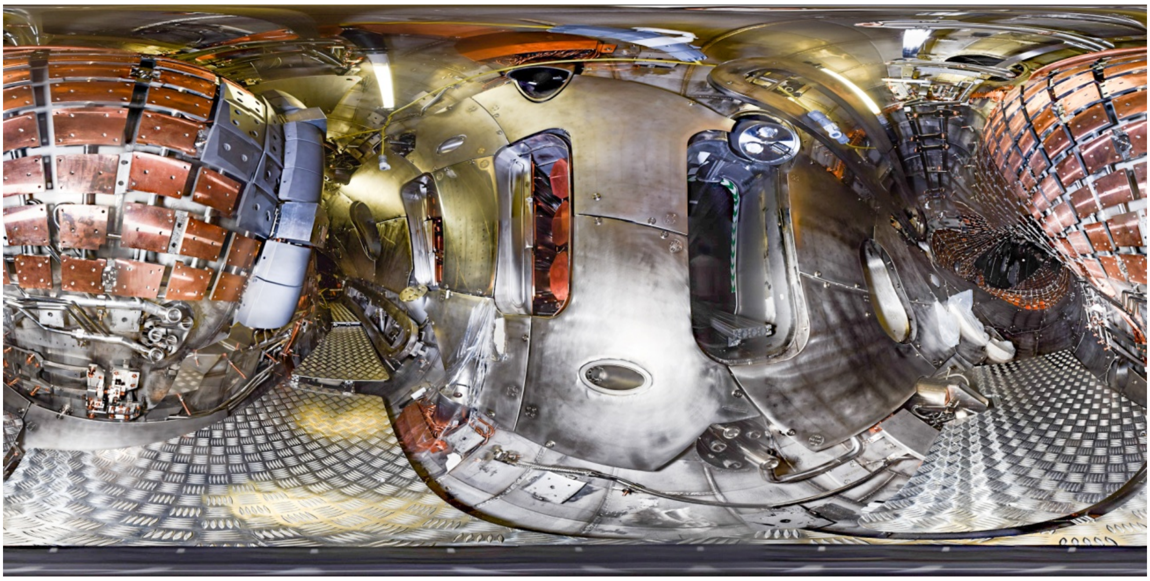

Figure 2. Panorama view: outer wall in module 5 (centre), left: module 5 in-board limiter (3rd tile from top and bottom, containing the limiter Langmuir probes, not yet installed).

of approx. 25000 × 12500 pixels (raw data size 3.2 GB). For quick full screen displaying also a strongly reduced resolution image of approx. 90 MB (figure 2) has been stored.

In addition to the panoramas, approx. 600 detailed photos per module were taken, which can be fitted into the panorama (by hand), if required, and used for even more detailed analysis.

The photo documentation was performed over a period of 2.5 months, always immediately after completion of the in-vessel works in the particular vessel modules, requiring one shift per module. The photo documentation will be repeated just after OP1.1 and just before OP1.2, then with the carbon tiles fitted to the heat shields and the TDU divertor installed.

2.2 Core plasma diagnostics

2.2.1 Neutron counters

Three neutron counter systems [9, 10] have been installed on W7-X, one sitting about 3.9 m above the centre of the torus at $R = 0$ m, while the two others are mounted on top of the cryostat vessel viewing the plasma in half modules 10 and 30. The central system consists of 5 counter tubes of different sensitivity to thermal neutrons, whereas the two peripheral ones contain 4 counter tubes, inserted in a specially designed moderator. The detectors have different sensitivities in order to allow measurement of the neutron yield of the plasma over more than five orders of magnitude with $< 15\%$ statistical uncertainty in time intervals of 5 ms. The design aims of the neutron monitors were confirmed by investigations in the reference radiation fields at the Physikalisch-Technische Bundesanstalt, Braunschweig, Germany, in 2014. In January 2015 they were calibrated at W7-X, using an in-vessel railway to transport a ^{241}Am/Be calibration source along the midplane of the plasma vessel. A relative standard uncertainty of $< 3\%$ has been achieved for the calibration factors, i.e. the ratio of the neutrons starting from the calibration source and the number of counts observed with the monitors.

2015 JINST 10 P10002

2.2.2 Flux surface measurements

Three flux surface measurement systems have been built, of which two have been installed in HM10 and HM30 for OP1.1. Each system consists of a scintillator coated rod with an electron gun at its tip. The specially designed drive allows full coverage of the roughly triangular shaped plasma vessel cross section and pulling back of the system behind an actively coolable shutter during plasma operation. For the observation of the fluorescent emission generated at the spot where the electron beam hits the rod, two PCO PixelFly cameras installed inside the AEQ21 and AEQ51 ports are being used. A spatial resolution of 2 mm will be achievable. As spatial reference, 4 metal-coated optical fibres were integrated into the wall structures in each plane, which are being illuminated from the outside of the plasma vessel. The measurements will start in May, i.e. right from the beginning of the commissioning of the superconducting coils, in order to learn how to correct any residual error fields with the trim coils and gather information how to correct for the effects resulting from the deformation of the coils with increasing field strengths [3].

2.2.3 Equilibrium magnetics and Mirnov coils

The major part of the magnetic diagnostics, consisting of 3 diamagnetic loops, 3 continuous and 5 segmented Rogowski coils, 40 saddle coils and 125 Mirnov coils, have been fully installed and will be available in OP1.1. [11] The diamagnetic loops are designed to resolve the plasma energy with an accuracy of 10 kJ (where the expected maximum value is $\sim$ 5 MJ) and a time resolution of better than 1 ms. The Rogowski coils are designed to measure the total toroidal plasma current with an accuracy of 100 A (where maximum net toroidal currents of $\sim$ 200 kA are predicted in certain discharge scenarios for the sum of bootstrap currents and microwave or neutral beam driven currents). The saddle coils and the segmented Rogowski coils deliver information to determine the poloidal and radial distribution of the toroidal current density (e. g., Pfirsch-Schlüter currents) in the framework of an equilibrium reconstruction. The Mirnov coils are arranged in three complete and one partial poloidal array with up to 41 coils in one array and will serve to resolve the poloidal mode structure of magnetic fluctuations, e.g., due to MHD modes. The low self-inductance, short signal cables, and their location behind gaps between the wall protection tiles will allow observing frequencies up to $\sim$ 1 MHz.

The design of all the installed magnetic diagnostics with their in-vessel signal cables is already suitable for long-pulse discharges, taking into account microwave stray radiation and further thermal loads from the back faces of wall protection elements, and the electronics and data acquisition modules are a special development for the numerical integration during discharges of up to 30 min [12].

2.2.4 Single channel dispersion interferometer

The line of sight averaged electron density will be provided by a single channel dispersion interferometer [13, 14] equipped with a Field Programmable Gate Array (FPGA) based data analysis. In OP1.1 we aim at demonstrating the real time capabilities of the W7-X dispersion interferometer set-up, [15, 16] but without the gas feedback loop yet being implemented. The time resolution for the line of sight integrated density measurements is 20 μs. The lower limit of the density measurements of about $3\,10^{17}$ m^{-2} to $\sim 1\,10^{18}$ m^{-2} is determined by the noise level and a gradual drift caused by air temperature and humidity induced dispersion variations, while at the upper end the first fringe jump will occur at $1.4\,10^{20}\,\mathrm{m}^{-2}$. The accuracy of the density measurements is about $\pm 3\,10^{17}\,\mathrm{m}^{-2}$. With the CO_2 (10.6 μm) and the frequency doubled laser beam (5.3 μm) line running collinear with the laser beam of the Thomson scattering diagnostic through the shared ports AET31, AEZ31 and the plasma centre, the line of sight averaged densities measured by the interferometer can also be directly used for cross calibration with the Thomson Scattering diagnostic.

2.2.5 Thomson Scattering

The $\sim$ 5–7 mm diameter beams of the two Nd-YAG lasers (repetition freq. 10 Hz at 4 J, 20 Hz at 2 J, 2 J/pulse, 10 ns pulse duration) pass through the oppositely located port pair AET31, AEZ31 and the plasma centre. The scattered light is being observed at an approximate angle of 90 degrees from two observation ports in the same plasma cross section (ports AEM31 and AEN31) [4]. In OP1.1 the observation optics in the AEM31 port is equipped only with ten optical fibres of two different lengths, providing a spatial resolution of 2 cm at the plasma centre and 3 cm at the edge, over the outer half profile. By making use of the time delay between the different fibre lengths, two fibres can be fitted to each of the five polychromators that are available in OP1.1. The polychromators consist of 1 Raman filter for calibration and 4 suitably selected filters to cover the temperature range from 20 eV to 10 keV and the density range from $5\,10^{18}\,\mathrm{m}^{-3}$ to $5\,10^{20}\,\mathrm{m}^{-3}$, both with an accuracy of $\sim 5\%$. The data acquisition system has a dynamic range of 12 bit and a time resolution of 1 ns.

2.2.6 Electron cyclotron emission (ECE) diagnostic

The electron temperature will be measured by a 32 channel Electron Cyclotron Emission (ECE) diagnostic applying a heterodyne radiometer followed by a filter bank [16]. A slim Gaussian beam characteristics with radius $w_0 = 20$ mm at its waist in the plasma centre, minimizes the emitting volume for each frequency interval, thereby maximizing the radial resolution. The filter bandwidth has been adapted to the optical depth of the corresponding emitting layers resulting in a radial resolution of 1 to 3 cm. An additional 16 channel zoom system selects a 4 GHz wide part of the spectrum at suitable radii using a tuneable second local oscillator at a second heterodyne stage. This span corresponds to a radial range of $\Delta r = 6$ cm at the high-field side or $\sim$ 15 cm at the low-field side. The zoom device is particularly dedicated to measuring the power deposition profile via heat wave analysis around the radius of the ECRH heating and to ELM studies. The standard time resolution of 100 kHz is blackbody noise limited to temperature fluctuations measurements of up to 1 MHz.

For in-situ calibration of the ECE system, a complete copy of the in-vessel optical system has been installed just outside the cryostat in air, allowing alternately probing the blackbody emission of two bodies at defined temperatures (77 K and room temperature). A waveguide switch integrated into the transmission line allows selection between the plasma observation and the calibration branch.

The above system is complemented by an additional small horn antenna, which is integrated into the heat shield, providing a view along the same line of sight from the high-field side, thereby allowing to also measure the emission from supra-thermal and current driven electrons. [16]

2.2.7 Electron cyclotron absorption (ECA) and stray radiation diagnostic

Especially in OP1.1, with starting W7-X for the very first time, initially relatively high impurity influx levels need to be expected and may lead to increasing strong energy losses and thereby decreasing electron temperatures in the course of a discharge, which could result in early discharge termination. To provide a means for an early detection of the transition towards such a scenario, the ECRH wall protection tiles opposite to the ECRH ports in module 1 and 5 (AEA11, AEE10, AEA51, AEE51) have been equipped with 2×63 open waveguide antennas. Each of them picks up a small part of the ECRH beam reaching the corresponding tiles and allows measuring the amplitude, polarization and position of the beam. Besides the determination of the power absorbed in the plasma, the electron cyclotron absorption (ECA) diagnostic can provide, for selected cases, the optical depth for the EC radiation at different radial positions, necessary for correcting the electron radiation temperatures determined by the ECE diagnostic for optically 'grey' plasmas ($T_e < 0.5$ keV, $n_e < 2 \cdot 10^{19}$ m^{-3}).

Furthermore, an ECRH stray radiation monitor, consisting of an oversized waveguide with a Schroeder diffusor in front of the detector providing a broad antenna characteristic, has been installed in each of the 5 vessel modules, to provide an interlock signal for the ECRH system, in case of unacceptably low plasma absorption. In addition, each of the 4 ECRH launchers is equipped with a NIR camera described in section 2.3.2. They should detect arcing on the protection tiles and thermal overloading in the long pulse discharges in OP2.

2.2.8 Reflectometer systems

Two reflectometer systems [16] are installed in port AEA21. The V-band hopping Doppler reflectometer (50–70 GHz), provided by CIEMAT, [17] is designed to resolve density fluctuations in the steep edge gradient region around $r/a = 0.85$–0.95 (~ 2.5 cm) with a fixed incidence angle (18°), which translates into a selected fluctuation wavelength of ~ 1 cm. The sampling frequency will initially be 10 Ms/s to be upgraded for OP1.2 to 20 Ms/s. The Ka-band poloidal correlation hopping reflectometer (25–50 GHz), provided by Forschungszentrum Jülich (FZJ), consists of an array of one launching and four receiving antennae [18], which observe density fluctuations around the separatrix ($r/a \sim 0.95$–1) sampled at 4 MHz. From the multiple antennae setup, parameters like propagation velocities, correlation lengths, and the local magnetic field pitch angle can be derived. The radial resolution of both instruments is in the range of a few millimetres, depending on the density gradient and the amplitude of the density fluctuations.

2.2.9 High resolution X-ray imaging system (HR-XIS)

The high resolution X-ray imaging system has been set up by FZJ [19]. The diagnostic provides line integrated measurements of standard plasma parameters like ion and electron temperatures, plasma rotation and argon impurity densities. Therefore, helium-like states of argon are monitored along one central and one line of sight across the lower half of the flux surfaces in a poloidal plane, with a spatial resolution of 2 cm. As detectors, two CCD cameras and optionally a gas detector can be used. Wavelength selection by Bragg-reflection ($\lambda = 4$ Å) is achieved with a spherically bent crystal, yielding an ion and electron temperature resolution of 90 eV, with an electron temperature range between 0.3 to 3 keV. Without binning, the CCD detector has a maximum time resolution of 100 ms, the gas detector achieves a time resolution of 25 ns. The inference of plasma parameter profiles from the line integrated measurements will be realised using a diagnostic forward model [20], implemented in the Minerva Bayesian analysis framework [21]. As an upgrade, the spectrometer allows to install up to 6 spherically bent crystals on a rotatable mount, giving access also to the highest ionization states of several other impurity species like e.g. iron or sulfor [22].

2.2.10 X-ray imaging crystal spectrometer (XICS)

The X-ray imaging crystal spectrometer [22] is being provided by PPPL, Princeton, U.S.A.. The XICS diagnostic will provide profiles of the ion-temperature T_i, electron-temperature T_e, poloidal flow velocity v_p and impurity ion density for the Ar^{16+} charge state [23]. Tomographic inversion, using a known plasma equilibrium, is used to infer the local plasma parameters from the line integrated data [24, 25]. This system will have a maximum time resolution of 5 ms, a spatial resolution of approximately 2 cm, and spatial coverage from the core to a normalized minor radius of $\rho \approx 0.82$. The diagnostic will be installed at the AEK31 port, which is a large radially viewing midplane port. A spherical quartz crystal, with a cut along the $(1,1,0)$ axis, will be used to provide dispersion and imaging of the plasma generated x-rays. For x-ray detection, the system will utilize a water cooled Pilatus 300K-W hybrid-pixel CMOS detector from Dectris Ltd.. The system is expected to measure T_e with a resolution of 20 eV, T_i with a resolution of 20 eV and v_p with a resolution of 5 km/s. To obtain sufficient signal for these measurements, an argon density of approximately $n_{\mathrm{Ar}}/n_e = 10^{-5}$ is required. Argon puffing will be achieved through the W7-X gas injection system or through the helium beam diagnostic system.

2.2.11 Pulse Height Analysis System (PHA)

The PHA system has been developed and manufactured at IPPLM, Warsaw [26], while support and infrastructure has been provided by IPP. Three silicon drift detectors equipped with different absorber foils are mounted in a vacuum chamber behind a set of 3 remotely controlled exchangeable filters with Be-foil thicknesses varying between 0 and 500 μm to record a wide range of x-ray energies with optimized resolution. An adaptable entrance aperture consisting of two crossed piezo-slits (max. width: 1.35 mm) allows to minimize degradation of the detector resolution at high intensities and optimal throughput at low intensity. This line of sight system with three different energy bandwidths is installed at port AEK50 and allows to determine Z_{eff}, measure various impurity species, the central electron temperature and investigate supra-thermal tails in the spectra over a cross section of $\sim 10 \times 10\,\mathrm{cm}^2$ with a time resolution of 100 ms, covering the energy range from 250 eV up to 20 keV with a resolution not worse than 200 eV (nominally 130 eV@5.9 keV) [27]. For in-situ calibration the commercial Mini-X X-ray tube from AMPTEK Inc. (4 – 48 keV at 50 kV/80 μA, Target: silver) has been integrated in the system. After passing through 1 mm Aluminium window (10 – 48 keV), the x-ray emission from this source, illuminates inside the vacuum chamber a stainless steel plate (also containing Cu and Ti), thereby inducing a fluorescent signal, suitable for calibration over the large energy range. For data acquisition a 4-channel digital X-ray processor, Mercury-4, from XIA LLC is being used.

2015 JINST 10 P10002

2.2.12 High Efficiency eXtreme ultraviolet Overview Spectrometer (HEXOS)

The HEXOS survey spectrometer system [22, 28, 29] consists of 4 VUV spectrometers with different incidence angles, ranging from near normal incidence (45 deg.) to grazing incidence (86 deg.). Two sets of two spectrometers are mounted in single frames back to back, in total covering the spectral range from 2.5 to 160 nm. The system has been provided by FZJ and has already been calibrated [30] and extensively tested on TEXTOR together with a W7-X Mini-CoDaC control and data acquisition system. The HEXOS device, which is installed in the plasma vessel midplane at the AEU10 port, will provide detailed spectral information in particular on the medium- and high-Z impurities. Each instrument is equipped with a linear diode array (1024 pixels) with an attached multi-channel plate image intensifier [31]. The time resolution of the detectors is 1 ms.

2.2.13 Horizontal and vertical bolometer systems

A horizontal and a vertical bolometer system [32], equipped with 32 and 40 channels, respectively, has been installed in the AEU30 and AEV21 ports, allowing tomographic reconstruction of the 2D emission profiles in the triangular shaped plane of W7-X. A spatial resolution of about 5 cm and a time resolution of 3 ms are expected for OP1.1. Additionally, on the secondary detector arrays of the two bolometer systems 8 channels, each covered with 10 μm-Be filter, are available for measuring the soft X-ray (> 800 eV) emission from the plasma centre.

2.2.14 Z_{eff} Bremsstrahlung measurement

In OP1.1 only a single line of sight Z_{eff} bremsstrahlung system is installed, looking radially through the plasma centre via optical windows in the port lids of the oppositely located ports AET40 and AEZ40. The light is being collected by a camera lens and then transported via a 1mm diameter optical fibre to a micro-spectrometer in the lab, covering the spectral range from 350 to 1000 nm with a time resolution of 5 ms. A Bayesian analysis procedure, in which the spectral lines are treated as nuisance parameters, will be used to derive Z_{eff} from the underlying background over the entire spectral range [33].

2.3 Edge and limiter plasma diagnostics

2.3.1 Video diagnostic

Ten video diagnostics systems [34] developed and provided by the Wigner Institute, Budapest, have been installed in all 10 AEQ ports, providing a toroidal view of the plasma and the entire plasma vessel wall. The price to pay to gain a toroidal view of the plasma is that the 10 cm diameter port bends around a coil. Therefore the EDICAM [35, 36] CMOS camera with its lens needs to be transported through the port, until it locks to a ring welded into the port close to the plasma vessel opening. This made it necessary to mount the vacuum window from the in-vessel side to the same welded ring inside the port. IPP has provided the diagnostics front end consisting of the window, a small uncooled shutter and a water cooled plasma facing front plate with a pinhole, which also forms the entrance pupil of the optics. The 1280×1024 pixel cameras provide a spatial resolution of 2 mm at all distances and a time resolution of 2.5 ms in full frame mode. The highly sophisticated features of the EDICAM system, of e.g. non-destructive and independent region-of-interest read-out possibilities, will not be made use of in OP1.1. The simultaneous control and display of all cameras in the control room will be provided by the VIDACS [36] program developed by the Wigner Institute.

Two of the ten systems (at the AEQ21 and AEQ51 ports) are in OP1.1 equipped with PCO PixelFly CCD cameras to allow a higher sensitivity of the flux surface measurements. To further improve the signal quality for these measurements, also a higher throughput lens is being used and at one port the water cooled pinhole plate has not yet been installed for this reason. At port AEQ30 a damaged bellow made it necessary to evacuate the entire port tube. To maintain the observation from this port, a fibre optic image guide consisting of 800×1000 fibres and an optic has been installed, instead of the EDICAM capsule, in the port bellow, to transport the light to the outside of the port, where depending on the experimental program either the EDICAM or the fast Photron SA5 camera from Wigner Institute will be installed.

2.3.2 2D NIR/visible limiter observation

10 immersion tube based systems with three observation windows at their plasma facing end and a rotating shutter blade in front are installed at the 10 AEF ports for later divertor observation in OP1.2. In the first campaign these systems will also provide a reasonable view of the 5 limiter tiles. Directly behind the windows 2 magnetic field compatible visible light cameras and one near infrared (NIR) camera are installed. The cameras are equipped with wide angle viewing optics, having a field of view of 86° or 136° and some with interference filters for H_α, CII, CIII radiation. The visible cameras (Raptor Photonics: CYGNET 2048×2048 pixels) and the NIR cameras (SONY XC-EI50CE: 768×494 pxl.), both have a time resolution of 40ms.

An additional immersion tube, equipped with the same NIR camera, has been integrated into each of the four ECRH launchers to monitor the temperature of the ECRH wall protection tiles and also the temperature distribution patterns on the limiters opposite to the launchers in modules 1 and 5. For the NIR cameras CEA has provided the software for camera control, data acquisition and storage of the data in the central data base.

Furthermore, port AEA30 has been equipped with a 216 mm diameter sapphire window for OP1.1, to allow high resolution nearly perpendicular observation of the central part of the limiter with a magnetically shielded, cooled 3–5 μm InSb IR camera (FLIR SC8303HD, 1344×768 pixels, 120 Hz frame rate, with a 200 mm f/4 lens) and a CMOS colour camera (Allied Vision Technologies Prosilica GX 1050 1024×1024 pixel, frame rate: 112 Hz) providing a spatial resolution of < 1 mm on the limiter surface.

2.3.3 Limiter integrated Langmuir probe arrays

In the 3rd tile from the top and bottom of the limiter in module 5 twenty Langmuir probe tips have been integrated, each, which will provide information on T_e, n_e, floating potential and the power decay length (λ_q) in the scrape-off layer. The Langmuir probes are cylindrical graphite tips with a diameter of 0.9 mm. The tips at the rim of the limiter are flush mounted, the other tips stick out of the limiter surface by about 1 mm. To measure the I/U-characteristics the bias-voltage can be swept between $+/-200$ V within a few milliseconds.

2.3.4 Neutral gas pressure measurements

Five ASDEX type neutral pressure gauges [37] have been installed in the midplane ports AEE11, AEE21, AEE30, AEE41 and AEE50. These hot-cathode ionisation gauges were specially designed for operation in strong magnetic fields, operation in noisy environments and are well shielded from the plasma. To shield the interior of the pressure gauges from ECRH stray radiation and to ensure a gas exchange time constant of 1 ms, the screening box is perforated by a large number of 0.7 mm dia. holes, providing in total an open area equivalent to a 5.6 mm dia. hole. The position and orientation of the manometers has been carefully selected to ensure that magnetic configuration changes and in particular also operation of the trim coils do not affect the measurements. From the measured neutral flux densities pressures in the range from ~ 0.1 mbar up to 10^{-6} mbar can be derived.

In addition a Penning gauge developed at the University of Madison, Wisconsin, has been installed at AEE41, which will allow to also measure the total neutral pressure and the partial pressures from spectroscopic analysis of the Penning discharge plasma. The system is quite comparable to the setup at TEXTOR [38] and LHD but is being improved towards higher sensitivity for the spectroscopic measurements. The main task of the system is to determine the helium partial pressure but other fractional neutral pressures of residual impurities like argon or nitrogen will be accessible, too. With helium being the main working gas in OP1.1, this campaign is ideally suited to gain first experience with this diagnostic. Also, the system will aid quantitative characterization of the wall conditioning procedure.

2.3.5 Multi-purpose manipulator

The multi-purpose manipulator [39] developed at the research centre in Jülich, Germany, is installed at the AEK40 mid-plane port. The fast reciprocating head will be equipped with Langmuir probes, magnetic sensors and a piezo-controlled impurity gas inlet. Exposition of material samples for plasma wall interaction research is foreseen as well. This system will in OP1.2 allow to probe in the standard iota = 1 configuration the flux tube which connects the two divertor thermal He-beams. Already in OP1.1 investigation of the edge topology is envisaged.

2.3.6 Thermal He (Ne) diagnostic neutral beam and observation systems

The divertor thermal He-beam [40] gas boxes with 5 nozzles have been fitted through the AEH30 and AEH51 ports and for OP1.1, fixed to the divertor frames, while in OP1.2 they will be integrated into the divertor [41]. With the divertor observation endoscopes being under development for OP1.2 at the research centre in Jülich, in OP1.1 a simplified observation system has been installed, consisting of a bundle of 10 optical fibres fitted to a photo lens mounted directly behind a window installed in the AEI51 port lid and the same set-up with a single fibre at AEI30, mainly for first tests with Neon [41]. This will allow gaining some first experience with the operation of the beams and the signal analysis. An accompanying effort at UW Madison targets on improving the atomic physics data set in particular towards high density, low temperature divertor conditions and initial attempts for validation are considered for OP1.1.

2015 JINST 10 P10002

3 Summary

Two years ago, in spring 2013, it was decided to introduce an additional step in starting up the Wendelstein 7-X device, the brief OP1.1 limiter operation phase, with the primary aim of an early commissioning and demonstration of the functionality of the major W7-X device components. This staggered approach allows remedying any possible deficiencies during the following year of completion of the in-vessel installations required for OP1.2, i.e. the fitting of the carbon tiles to the heat shields and the installation of the uncooled divertor. It has been possible to complete already about half the diagnostics foreseen for the OP1.2 campaign in time for the early OP1.1 campaign, this providing also these diagnostics the opportunity of an early first operation. Moreover, by suitably re-prioritising the work, it was possible to complete a set of diagnostics that will allow running a short dedicated limiter plasma physics program. The total number, and in particular the individual priority of these diagnostics, had been defined at the time OP1.1 was conceived, taking into account the available resources, and the in-vessel assembly logistics. However, non-diagnostic in-vessel component installation sequences had to be changed a few times, and the diagnostic priorities and installation plans had to be updated accordingly, often at very short notice. The in-vessel and in-torus-hall installations were completed in time for first plasma operation, for the rather large set of diagnostics described here. A significant set of diagnostics still remains to be completed till the start or the middle of OP1.2. Some of them are already close to completion at IPP or at our external partners; others requiring to be installed together with the divertor. The remaining diagnostics being prepared for OP1.2 are: the first two of 10 for OP2 required long pulse compatible infrared/visible endoscopes for divertor temperature control, the diagnostic neutral beam injector RuDI-X together with the visible charge exchange and beam emission observation systems, as well as 3 active neutral particle analysers all looking at diagnostic neutral beam, the in-vessel integrated 400 channel soft x-ray multi-camera tomography system, a planned extension of the Thomson Scattering system to a full profile with 2.5 cm radial resolution, the first 4 channels of the multi-channel interferometer system, the multi-foil spectroscopy system, the Z_{eff} Bremsstrahlungs profile system, the profile reflectometry, the soft x-ray high sensitivity boron, carbon, oxygen and nitrogen monitor, the laser blow-off system, the 60 keV lithium beam and its observation systems, the impurity pellet system, phase contrast imaging diagnostic (PCI), several ECRH stray radiation bolometers, several exchangeable divertor target fingers for plasma wall interaction studies, divertor target integrated Langmuir probes, divertor thermo-couples, 4 divertor spectroscopy endoscopes systems, a divertor laser induced fluorescence system (LIF), various Halpha single lines of sight and additional neutral gas pressure measurement systems.

Acknowledgments

This work has been carried out within the framework of the EUROfusion Consortium and has received funding from the Euratom research and training programme 2014–2018 under grant agreement No 633053. The views and opinions expressed herein do not necessarily reflect those of the European Commission.

2015 JINST 10 P10002

References

[1] T. Klinger et al., *Towards assembly completion and preparation of experimental campaigns of Wendelstein 7-X in the perspective of a path to a stellarator fusion power plant*, Fusion Eng. Des. **88** (2013) 461.

[2] H.S. Bosch et al., *Technical challenges in the construction of the steady-state stellarator Wendelstein 7-X*, Nucl. Fusion **53** (2013) 126001.

[3] H.S. Bosch et al., *Transition From Construction to Operation Phase of the Wendelstein 7-X Stellarator*, IEEE Trans. Plasma Sci. **42** (2014) 432.

[4] R. König et al., *Diagnostics design for steady-state operation of the Wendelstein 7-X stellarator*, Rev. Sci. Instrum. **81** (2010) 10E133.

[5] R. König et al., *Diagnostics development for quasi-steady-state operation of the Wendelstein 7-X stellarator (invited)*, Rev. Sci. Instrum. **83** (2012) 10D730.

[6] R. König et al., *Status of the diagnostics development for the first operation phase of the stellarator Wendelstein 7-X*, Rev. Sci. Instrum. **85** (2014) 11D818.

[7] M. Hirsch et al., *Major results from the stellarator Wendelstein 7-AS*, Plasma Phys. Contr. F. **50** (2008) 053001, (see p. 64).

[8] T.S. Pedersen, *Plans for first plasma operation of W7-X*, *Stellarator News* **145** (2014) 1, http://web.ornl.gov/sci/fed/stelnews/pdf/sn145.pdf.

[9] ATLAS collaboration, *Development of a readout link board for the demonstrator of the ATLAS Tile calorimeter upgrade*, 2013 *JINST* **8** C03025.

[10] B. Wiegel et al., *Monitoring of the neutron production at the Wendelstein 7-X stellarator*, Radiat. Prot. Dosim. **161** (2014) 326.

[11] M. Endler et al., *Engineering Design for the Magnetic Diagnostics of Wendelstein 7-X*, Fus. Eng. Des. **100** (2015) 468.

[12] A. Werner, et al., *W7-X magnetic diagnostics: Performance of the digital integrator*, Rev. Sci. Instrum. **77** (2006) 10E307.

[13] P.A. Bagryanski et al., *Dispersion interferometer based on a CO_2 laser for TEXTOR and burning plasma experiments*, Rev. Sci. Instrum. **77** (2006) 053501.

[14] T. Akiyama et al., *Development of a dispersion interferometer for magnetic confinement plasma and its application to high-pressure plasmas*, in proceedings of the 1st *EPS conference on Plasma Diagnostics*.

[15] P. Kornejew et al., *Density Measurements at Fusion Experiments: 2-Color versus Dispersion Interferometer*, to be published.

[16] M. Hirsch et al., *Microwave and Interferometer Diagnostics prepared for first Plasma Operation of WENDELSTEIN 7-X*, in proceedings of the 1st *EPS conference on Plasma Diagnostics*.

[17] T. Happel, T. Estrada, E. Blanco, V. Tribaldos, A. Cappa and A. Bustos, *Doppler reflectometer system in the stellarator TJ-II*, Rev. Sci. Instrum. 80 (2009) 073502.

[18] A. Kraemer-Flecken et al., *Correlation reflectometry at TEXTOR*, Rev. Sci. Instrum. **81** (2010) 113502.

[19] G. Bertschinger, W. Biel, H. Jaegers et al., *Compact imaging Bragg spectrometer for fusion devices*, Rev. Sci. Instrum. **75** (2004) 3727.

[20] A. Langenberg et al., *Forward modeling of a high resolution X-ray imaging crystal spectrometer for the Wendelstein 7-X stellarator*, *Europhysics Conference Abstracts* **38F** (2014) P1.074, *41st EPS Conference on Plasma Physics*, http://ocs.ciemat.es/EPS2014PAP/pdf/P1.074.pdf.

[21] J. Svensson and A. Werner, *Large scale Bayesian data analysis for nuclear fusion experiments*, in proceedings of *2007 IEEE International Symposium on Intelligent Signal Processing* (2007) 955.

[22] H. Thomsen, *Startup impurity diagnostics in Wendelstein 7-X stellarator foreseen in the first operational phase*, in proceedings of the 1st *EPS conference on Plasma Diagnostics*.

[23] N. Pablant et al, *Measurement of core plasma temperature and rotation on W7-X made available by the x-ray imaging crystal spectrometer (XICS)*, *Europhysics Conference Abstracts* **38F** (2014) P1.076, *41st EPS Conference on Plasma Physics*, http://ocs.ciemat.es/EPS2014PAP/pdf/P1.076.pdf.

[24] N. Pablant. et al., *Tomographic inversion techniques incorporating physical constraints for line integrated spectroscopy in stellarators and tokamaks*, *Rev. Sci. Instrum.* **85** (2014) 11E424.

[25] A. Langenberg et al., *Inference of Temperature and Density Profiles via Forward Modeling of an X-ray Imaging Crystal Spectrometer within the Minerva Bayesian Analysis Framework*, submitted to *Rev. Sci. Instrum.*

[26] M. Kubowska et al., *Laboratory tests of the Pulse Height Analysis system for Wendelstein 7-X*, in proceedings of the 1st *EPS conference on Plasma Diagnostics*.

[27] S. Jabłonski et al., *Simulation of PHA Soft X-Ray Spectra Expected from W7-X*, in proceedings of the 1st *EPS conference on Plasma Diagnostics*.

[28] W. Biel et al., *Design of a high-efficiency extreme ultraviolet overview spectrometer system for plasma impurity studies on the stellarator experiment Wendelstein 7-X*, *Rev. Sci. Instrum.* **75** (2004) 3268.

[29] W. Biel, et al., *High efficiency extreme ultraviolet overview spectrometer: Construction and laboratory testing*, *Rev. Sci. Instrum.* **77** (2006) 10F305.

[30] A. Greiche et al, *Absolute intensity calibration of the Wendelstein 7-X high efficiency extreme ultraviolet overview spectrometer system*, *Rev. Sci. Instrum.* **79** (2008) 093504.

[31] W. Biel et al, *Detector system with high time resolution for the continuous measurement of spectra in the vacuum ultraviolet wavelength range*, *Rev. Sci. Instrum.* **75** (2004) 2471.

[32] D. Zhang et al., *Design criteria of the bolometer diagnostic for steady-state operation of the W7-X stellarator*, *Rev. Sci. Instrum.* **81** (2010) 10E134.

[33] M. Krychowiak et al, *Bayesian analysis of the effective charge from spectroscopic bremsstrahlung measurement in fusion plasmas*, *J. Appl. Phys.* **96** (2004) 4784.

[34] G. Kocsis et al., *Overview video diagnostics for the W7-X stellarator*, *Fusion Eng. Des.* **96-97** (2015) 808.

[35] A. Szappanos et al., *EDICAM fast video diagnostic installation on the COMPASS tokamak*, *Fusion Eng. Des.* **85** (2010) 370.

[36] S. Zoletnik, et el., *EDICAM (Event Detection Intelligent Camera)*, *Fusion Eng. Des.* **88** (2013) 1405.

[37] G. Haas and H.-S. Bosch, *In Vessel Pressure Measurement in Nuclear Fusion Experiments with ASDEX Gauges*, *Vacuum* **51** (1998) 39.

[38] T. Denner, K.H. Finken and G. Mank, *Helium partial pressure measurement in a deuterium environment*, *Rev. Sci. Instrum.* **67** (1996) 3515.

2015 JINST 10 P10002

[39] O. Neubauer et al., *Diagnostic setup for investigation of plasma wall interactions at Wendelstein 7-X*, *Fusion Eng. Des.* accepted for publication (2015).

[40] O. Schmitz, et al., *Status of electron temperature and density measurement with beam emission spectroscopy on thermal helium at TEXTOR*, *Plasma Phys. Contr. F.* **50** (2008) 115004.

[41] M. Krychowiak et al., *Bayesian modelling of a thermal helium beam for measurement of electron density and temperature in the W7-X divertor plasma*, *Plasma Phys. Contr. F.* **53** (2011) 035019.